chemosensors

MDPI

Article

Colorimetric and Fluorescence-Based Detection of Mercuric Ion Using a Benzothiazolinic Spiropyran

Ajeet Kumar, Arvind Kumar, Priya Ranjan Sahoo and Satish Kumar *

Department of Chemistry, St. Stephen's College, University Enclave, Delhi 110007, India

* Correspondence: satish@ststephens.edu

Supplementary Material

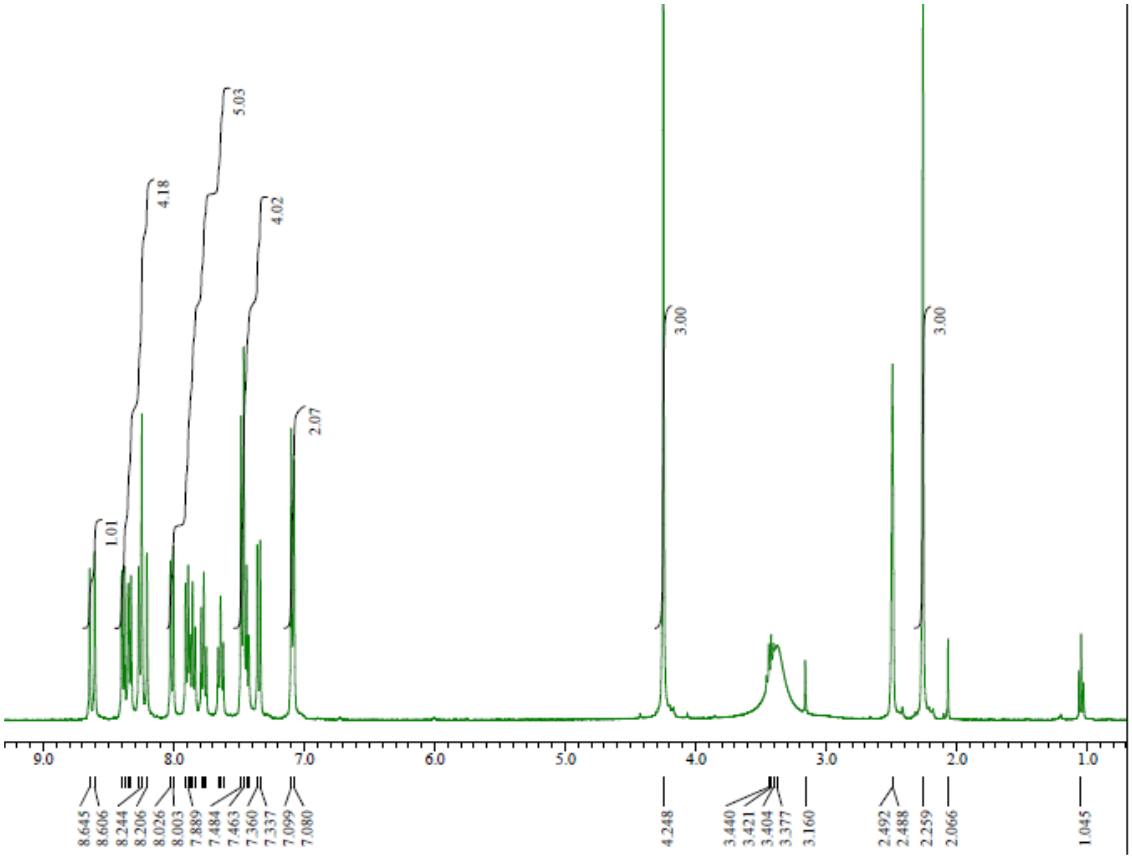

Figure S1. The ^{1}H-NMR of **1** recorded in DMSO-d_6 on a 400 MHz instrument.

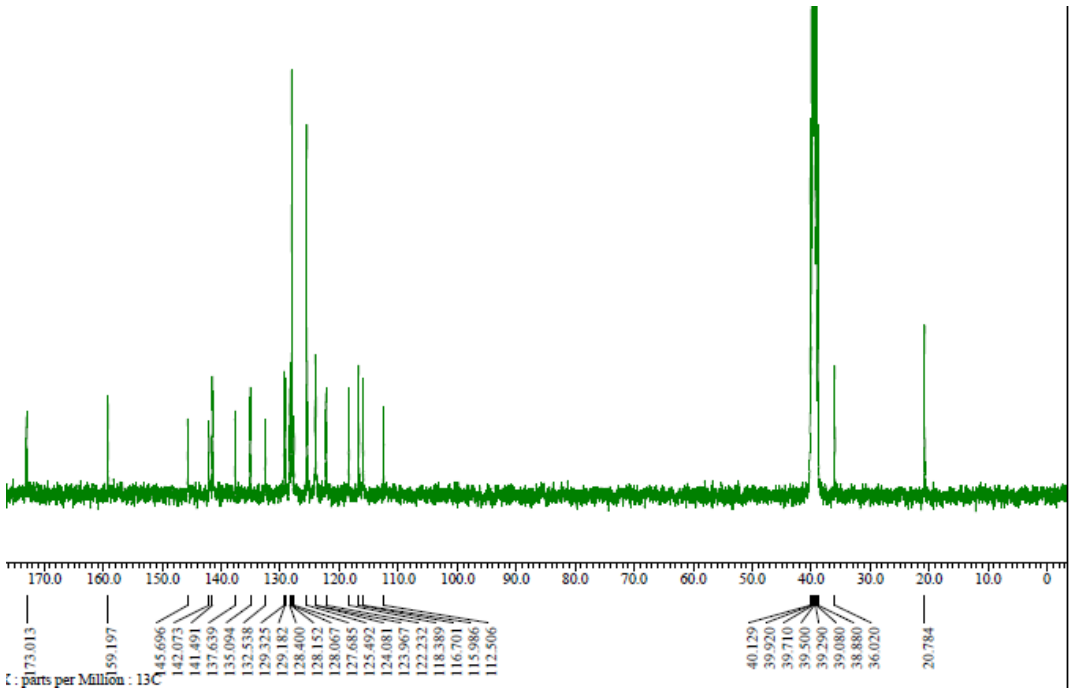

Figure S2. The ^{13}C-NMR of **1** recorded in DMSO-d_6 on a 400 MHz instrument.

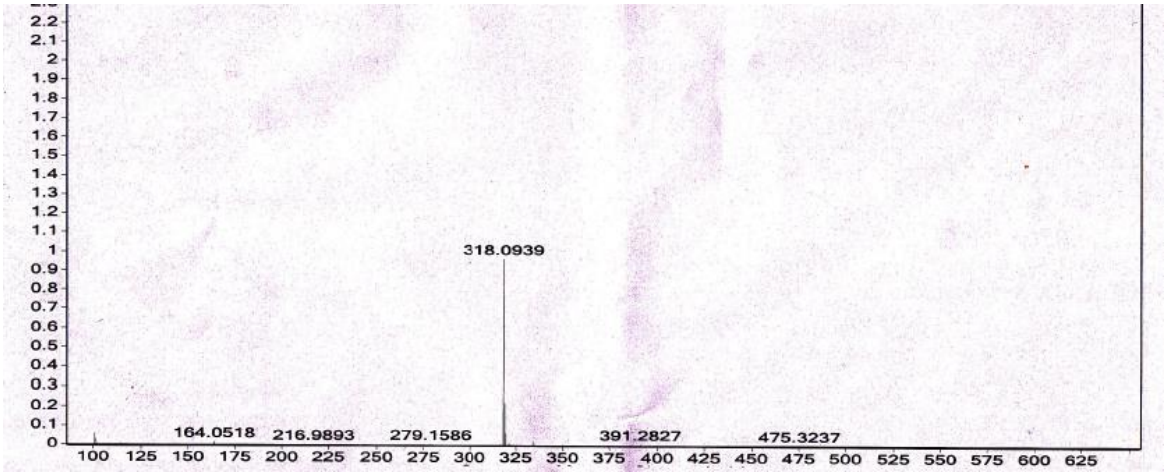

Figure S3. HR-MS of **1**. Calculated for $C_{20}H_{15}NOS^+$ (*m*/*z*): 318.0947; found 318.0939.

Table S1. Experimental detail.

	1
CCDC	1870439
Crystal data	
Chemical formula	$C_{20}H_{16}NOS{\cdot}C_7H_7O_3S$
M_r	489.58
Crystal system, space group	Monoclinic, $P2_1/c$
Temperature (K)	293
a, *b*, *c* (Å)	7.1366 (9), 15.2998 (15), 21.7465 (19)
β (°)	98.408 (10)
V (Å^3)	2349.0 (4)
Z	4
Radiation type	Mo$K\alpha$
μ (mm^{-1})	0.26
Crystal size (mm)	0.02 × 0.01 × 0.01
Data collection	
Diffractometer	Xcalibur, Sapphire3
Absorption correction	Multi-scan, *CrysAlis PRO, 2015*
T_{min}, T_{max}	0.134, 1.000
No. of measured, independent and observed [$I > 2\sigma(I)$] reflections	9378, 3356, 1186
R_{int}	0.276
$(\sin\theta/\lambda)_{max}$ (Å^{-1})	0.594
Refinement	
$R[F^2 > 2\sigma(F^2)]$, $wR(F^2)$, *S*	0.092, 0.181, 0.82
No. of reflections	3356
No. of parameters	312
H-atom treatment	H atoms treated by a mixture of independent and constrained refinement
$\Delta\rho_{max}$, $\Delta\rho_{min}$ (e Å^{-3})	0.36, −0.25

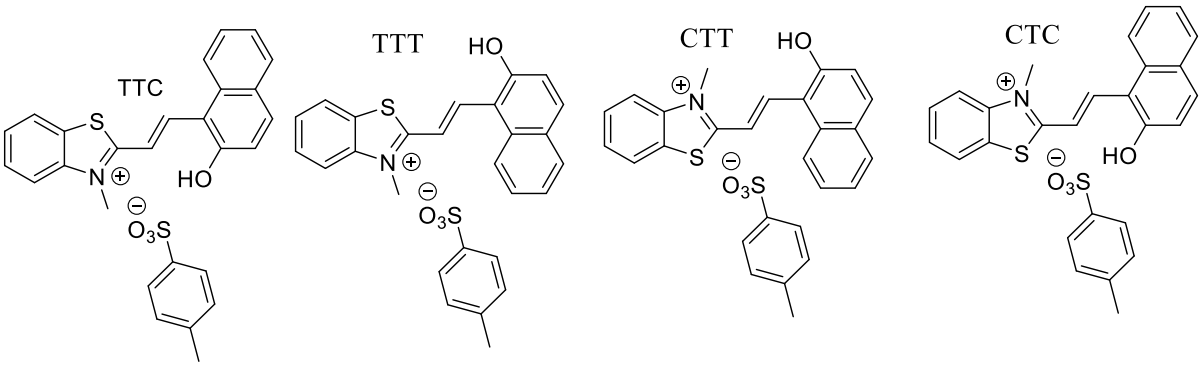

Figure S4. The structure of different stereoisomers of **1**.

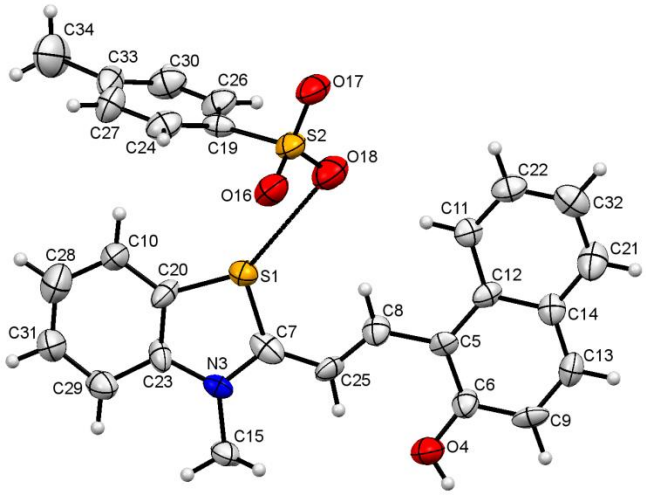

Figure S5. The crystal structure of **1** showing O···S and C-H···O interactions.

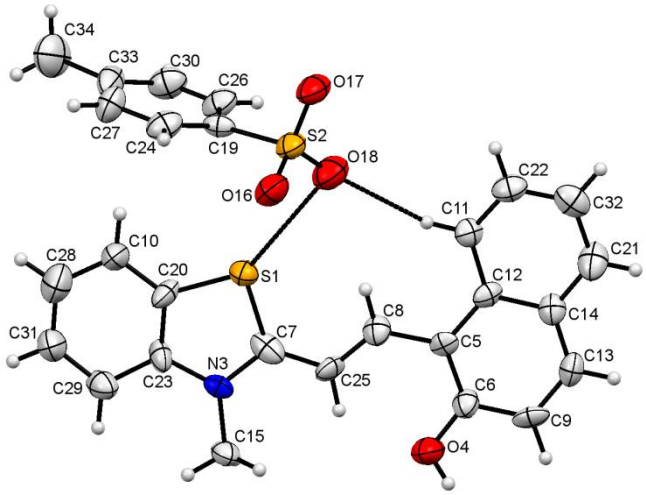

Figure S6. The crystal structure of **1** showing O····S interaction.

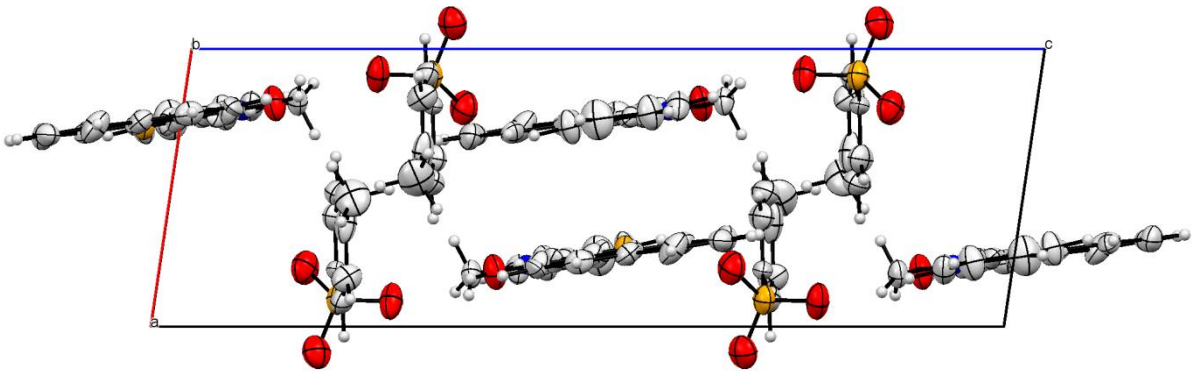

Figure S7. The crystal packing diagram of **1** viewed along b-axis showing the packing of receptor units in the lattice with the help of H-bonds.

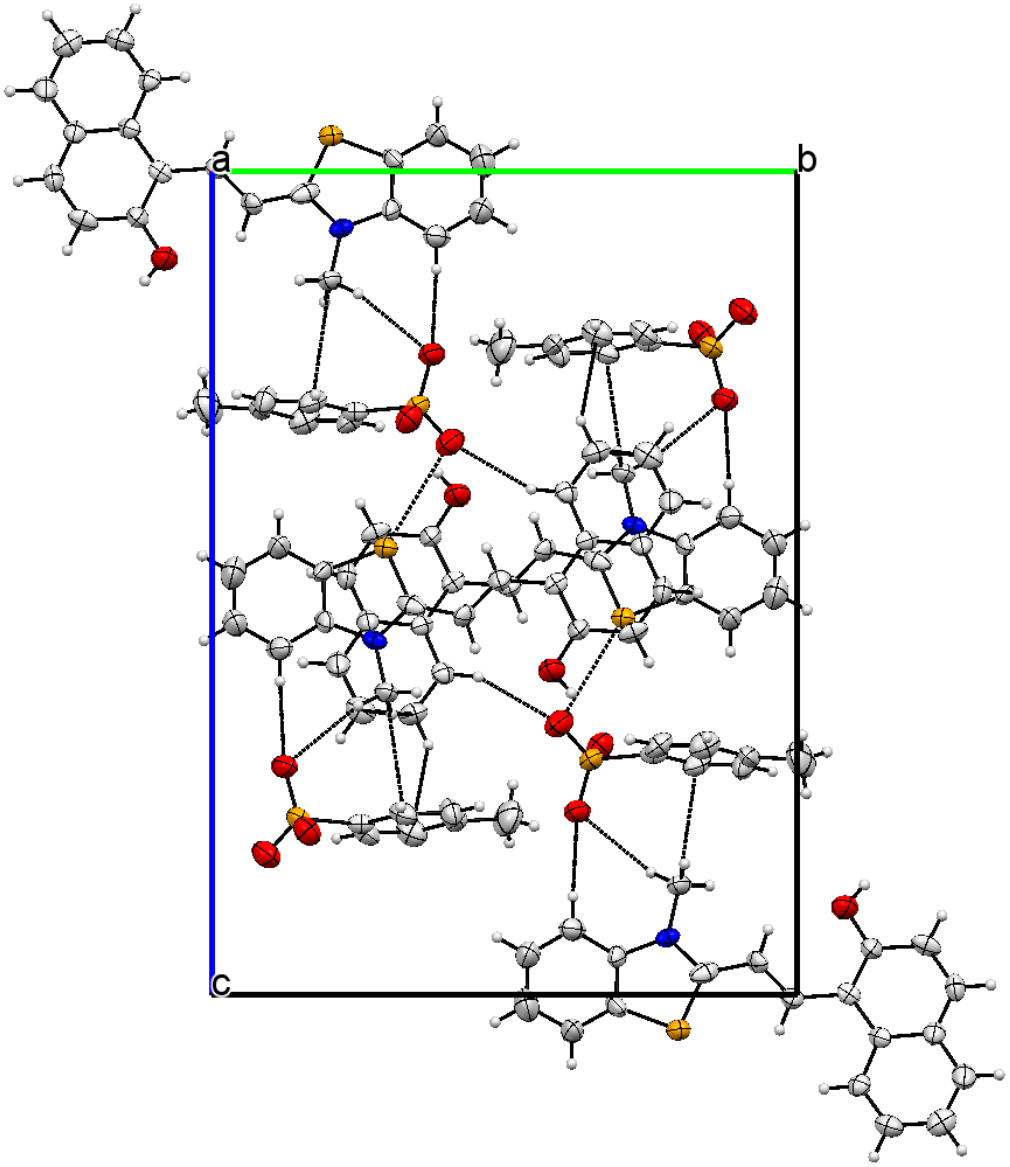

Figure S8. The crystal packing diagram of **1** viewed along a-axis showing short intermolecular contacts.

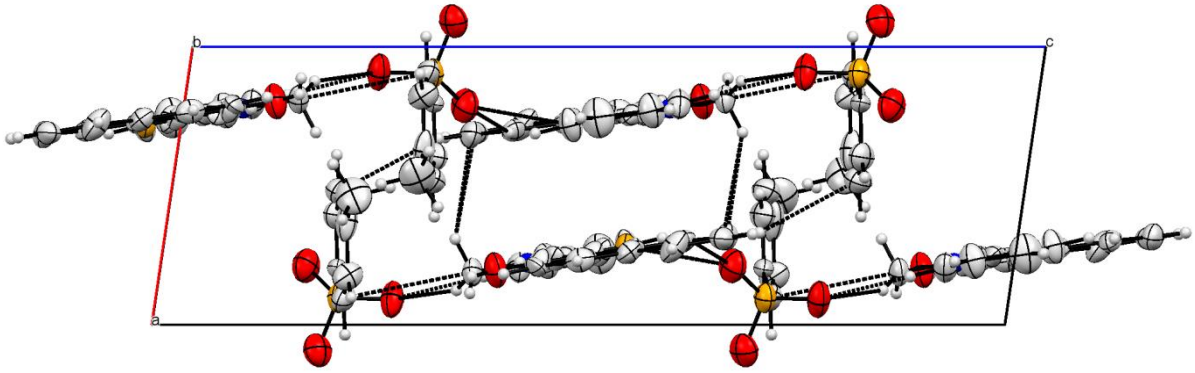

Figure S9. The crystal packing diagram of **1** viewed along b-axis showing short intermolecular contacts.

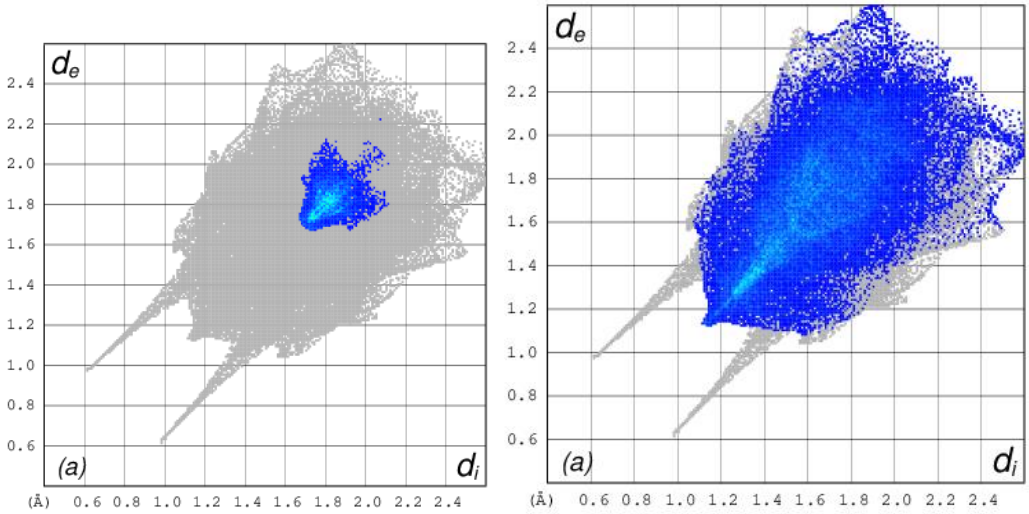

Figure S10. 2D Fingerprint plots of **1** showing (a) C···C (b) H···H contacts.

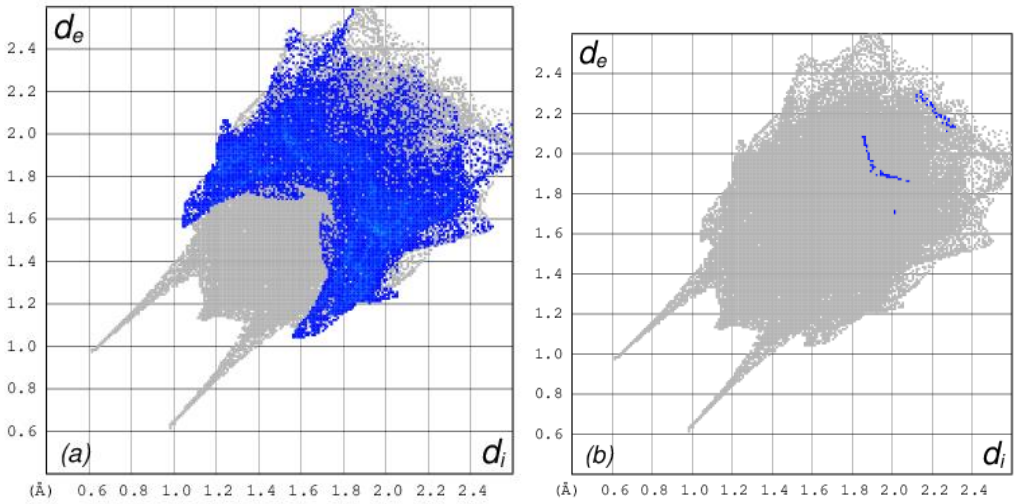

Figure S11. 2D Fingerprint plots of **1** showing (a) C···H (b) C···O contacts.

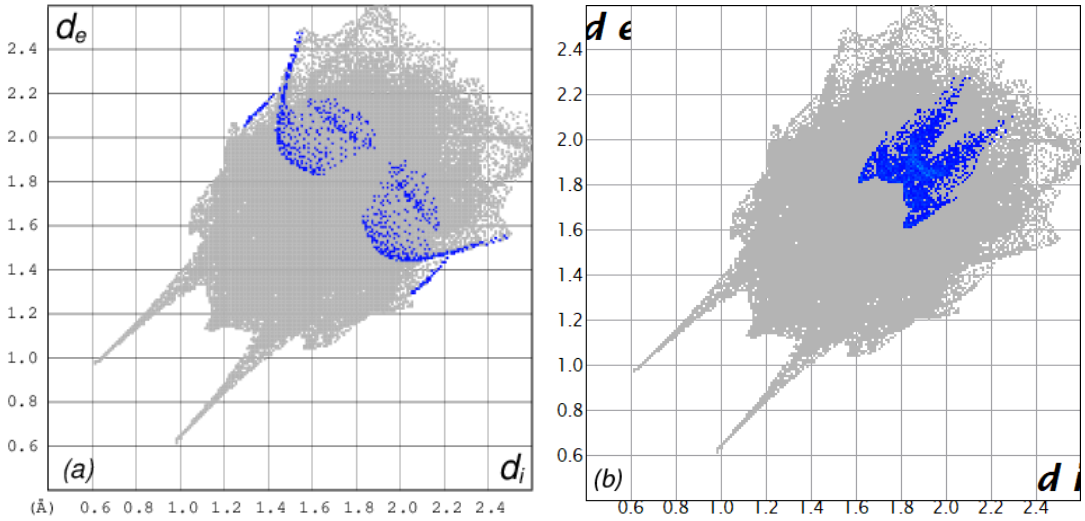

Figure S12. 2D Fingerprint plots of **1** showing (a) S···H and (b) S···C contacts.

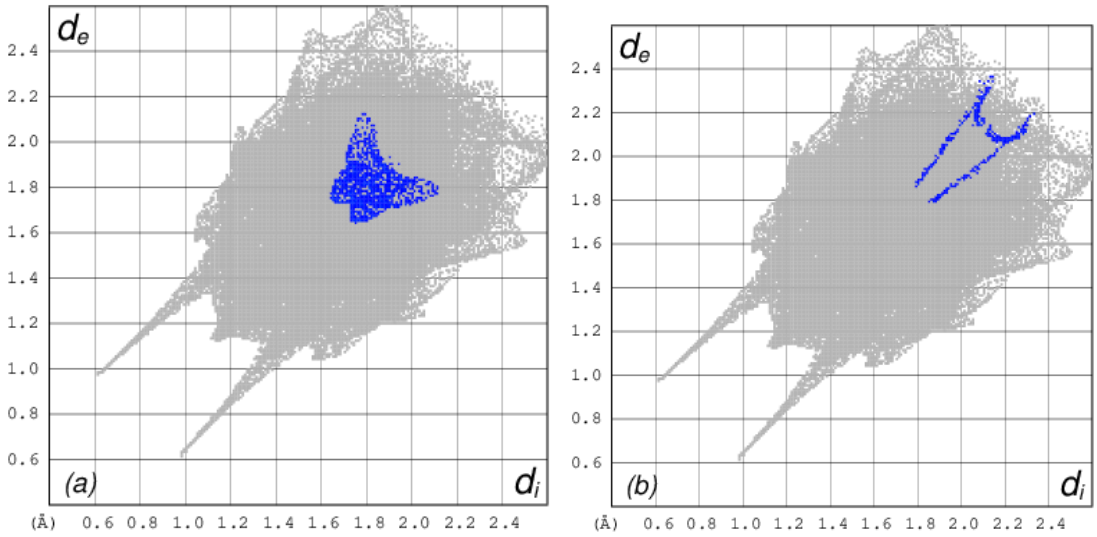

Figure S13. 2D Fingerprint plots of **1** showing (a) C···N (b) O···O contacts.

Table S2. contribution of different intermolecular interaction to the total Hirshfeld surface.

C-C	C-H	H-H	C-N	C-O	O-H	O-O	S-C	S-H
6.6	22	44.7	1.4	0.1	21	0.3	3	0.9

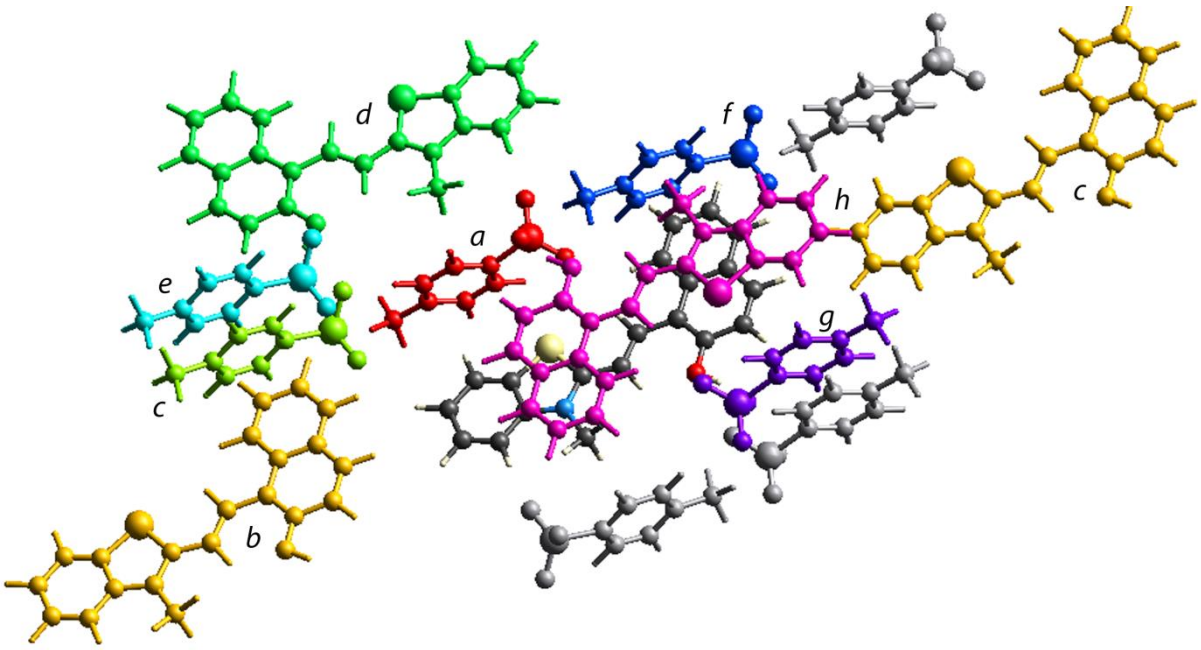

Figure S14. The interaction of central merocyanine unit with other molecular units obtained using Crystal Explorer program.

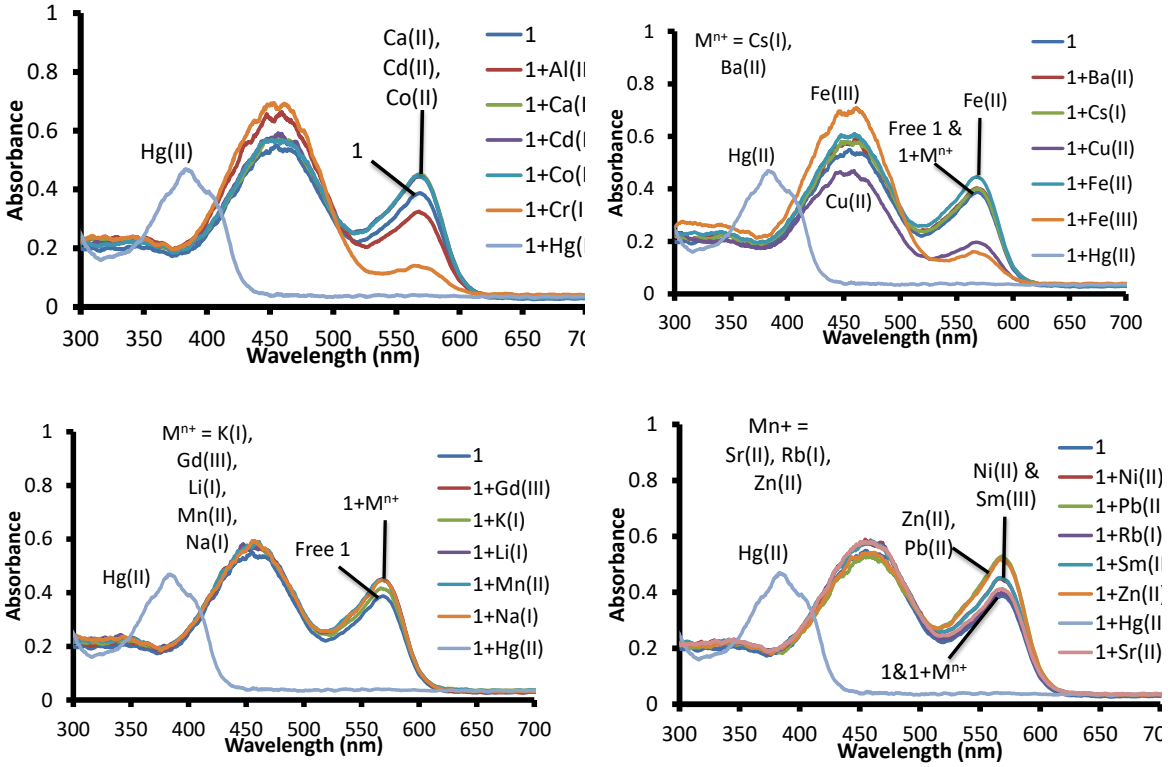

Figure S15. An expanded view of the change in absorption spectra of solutions of receptor **1** in water (pH=7.6, 1.0 mM HEPES) upon addition of acetate salts of different metal ions. [**1**] = 20 μM = [M^{n+}] = Hg^{2+}, Na^{+}, K^{+}, Li^{+}, Cr^{3+}, Al^{3+}, Fe^{3+}, Mn^{2+}, Ni^{2+}, Pb^{2+}, Zn^{2+}, Co^{2+}, Cu^{2+}, Cs^{+}, Ba^{2+}, Sr^{2+} ions.

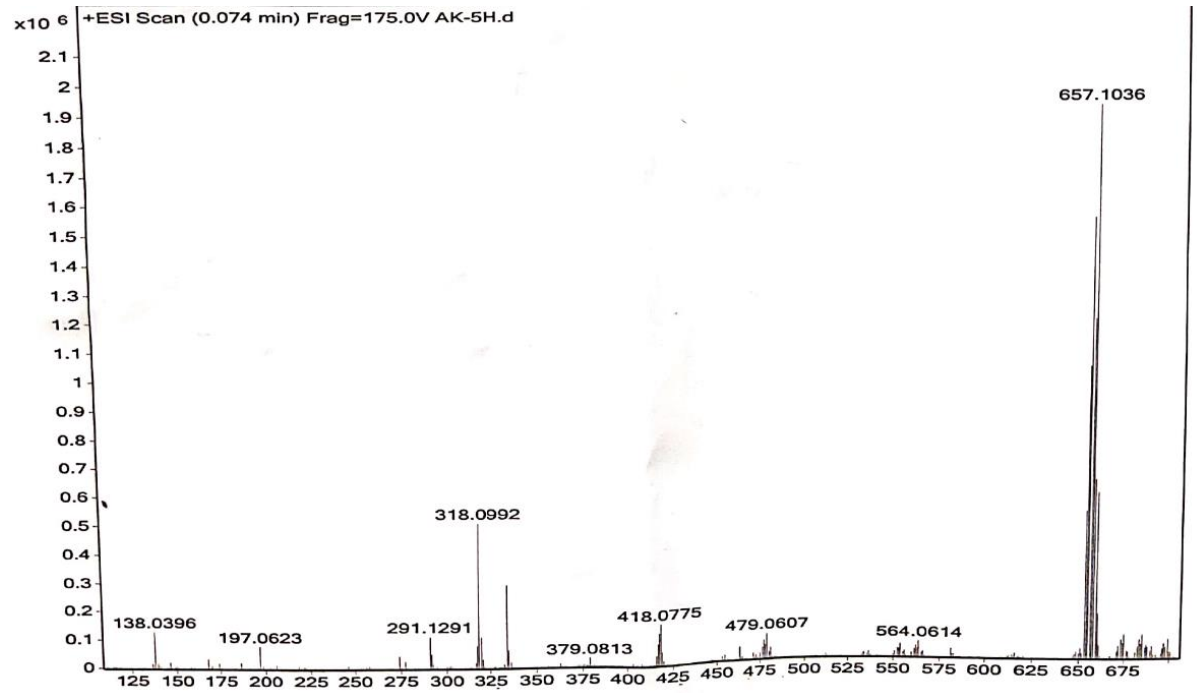

Figure S16. The HR-MS of a solution of **1**-Hg^{2+} prepared in acetonitrile.

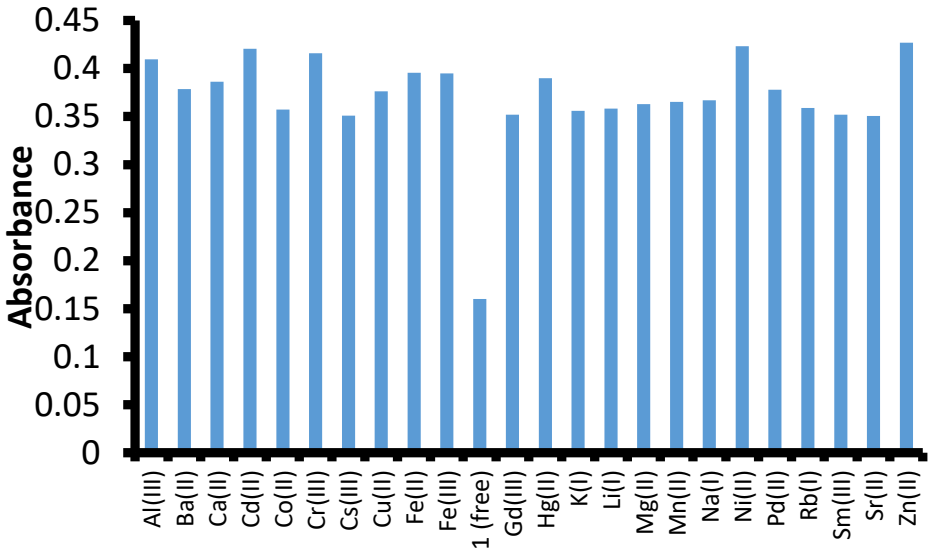

Figure S17. The bar chart drawn at 375 nm for **1** (20 μM) upon addition of one equivalent mercuric ion and one equivalent different metal ions to a solution of **1** in water (1.0 mM HEPES, pH 7.6).

Figure S18. Color change in the solutions of receptor **1** (20 μM) in water (pH = 7.6, 1.0 mM HEPES) upon addition of acetate salts of various metal ions in the presence of the same concentration of other metal ion. [**1**] = 20 μM = [M^{n+}]. From left to right, A = Free, B= Hg^{2+}, C=Hg^{2+}+Al^{3+}, D= Hg^{2+}+Cr^{3+}, E= Hg^{2+}+Fe^{3+}, F= Hg^{2+}+Cu^{2+}, G= Hg^{2+}+Rb^{+}, H= Hg^{2+}+Sm^{3+}, I = Hg^{2+}+Zn^{2+}, J = Hg^{2+}+K^{+}, K = Hg^{2+}+Gd^{3+}, L = Hg^{2+}+Pb^{2+}, M = Hg^{2+}+Ca^{2+}, N = Hg^{2+}+Ni^{2+}, O = Hg^{2+}+Cd^{2+}, P= Hg^{2+}+Fe^{2+}, Q= Hg^{2+}+Mg^{2+}, R = Hg^{2+}+Pd^{2+}, S = Hg^{2+}+Na^{+}, T = Hg^{2+}+Cs^{+}, U = Hg^{2+}+Li^{+}, V= Hg^{2+}+Ba^{2+}, W = Hg^{2+}+Co^{2+}, X = Hg^{2+}+Sr^{2+}.

Figure S19. Color change on paper strips coated with the receptor **1,** dipped in the solutions of acetate salts of various metal ions in the presence of the same concentration of other metal ion. [**1**] = 20 μM = [M^{n+}]. From left to right, A = Free, B= Hg^{2+}, C=Hg^{2+}+Al^{3+}, D= Hg^{2+}+Cr^{3+}, E= Hg^{2+}+Fe^{3+}, F= Hg^{2+}+Cu^{2+}, G= Hg^{2+}+Rb^{+}, H= Hg^{2+}+Sm^{3+}, I = Hg^{2+}+Zn^{2+}, J = Hg^{2+}+K^{+}, K = Hg^{2+}+Gd^{3+}, L = Hg^{2+}+Pb^{2+}, M = Hg^{2+}+Ca^{2+}, N = Hg^{2+}+Ni^{2+}, O = Hg^{2+}+Cd^{2+}, P= Hg^{2+}+Fe^{2+}, Q= Hg^{2+}+Mg^{2+}, R = Hg^{2+}+Pd^{2+}, S = Hg^{2+}+Na^{+}, T = Hg^{2+}+Cs^{+}, U = Hg^{2+}+Li^{+}, V= Hg^{2+}+Ba^{2+}, W = Hg^{2+}+Co^{2+}, X = Hg^{2+}+Sr^{2+}.

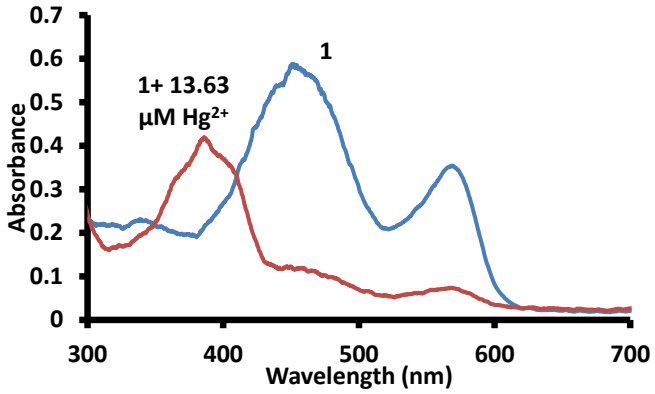

Figure S20. Change in absorption spectra upon addition of 13.63μM mercuric ions in a solution of **1** (20 μM) in water at pH 7.0 (1.0 mM HEPES).

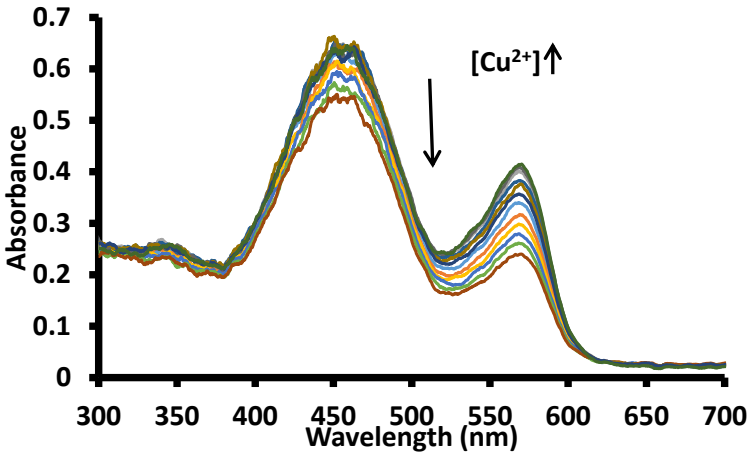

Figure S21. Change in absorption spectra during titration of **1** ([**1**] = 20 μM) with copper ions in water at pH 7.0 (1.0 mM HEPES).

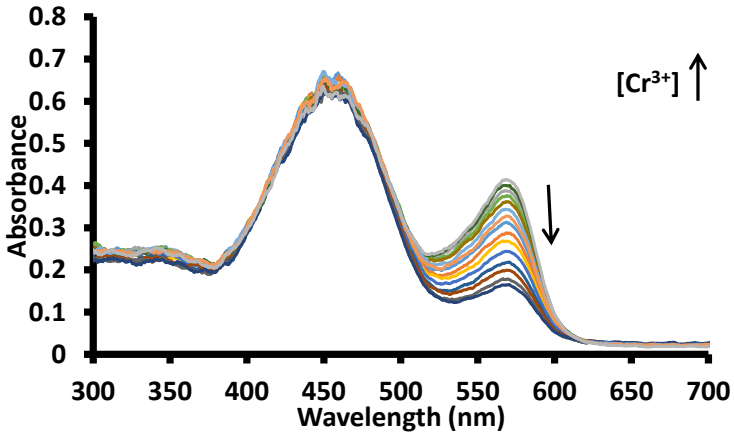

Figure S22. Change in absorption spectra during titration of **1** ([**1**] = 20 μM) with chromium ions in water at pH 7.0 (1.0 mM HEPES).

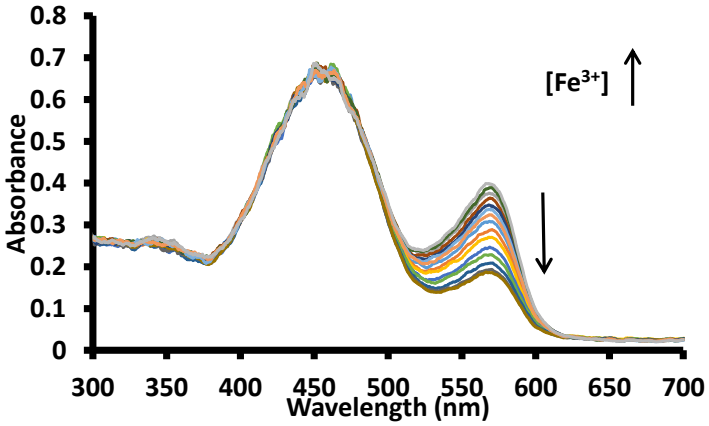

Figure S23. Change in absorption spectra during titration of **1** ([**1**] = 20 μM) with ferric ions in water at pH 7.0 (1.0 mM HEPES).

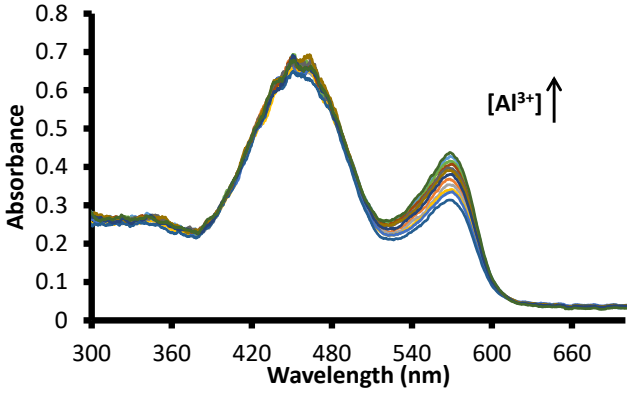

Figure S24. Change in absorption spectra during titration of **1** ([**1**] = 20 μM) with aluminum ions in water at pH 7.0 (1.0 mM HEPES).

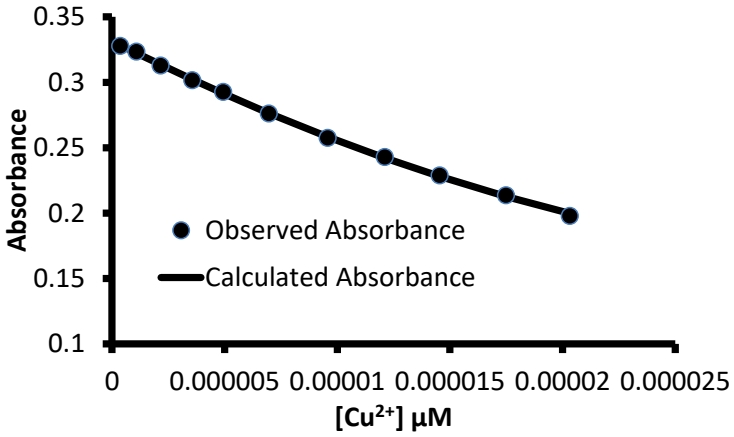

Figure S25. A correlation between the observed absorbance and absorbance value calculated using the HypSpec program for a titration between **1** and copper ions with 1:1 (H:G) binding stoichiometry.

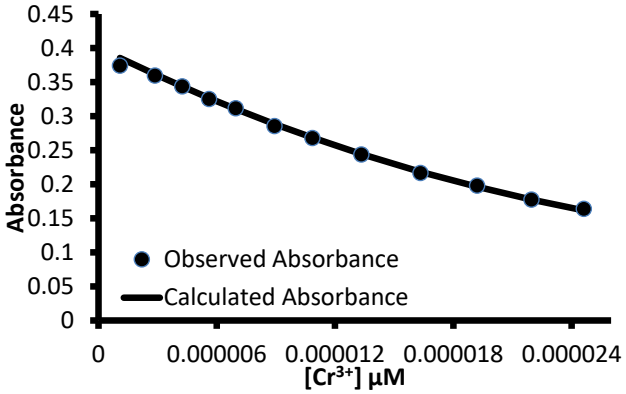

Figure S26. A correlation between the observed absorbance and absorbance value calculated using the HypSpec program for a titration between **1** and chromium ions with 1:1 (H:G) binding stoichiometry.

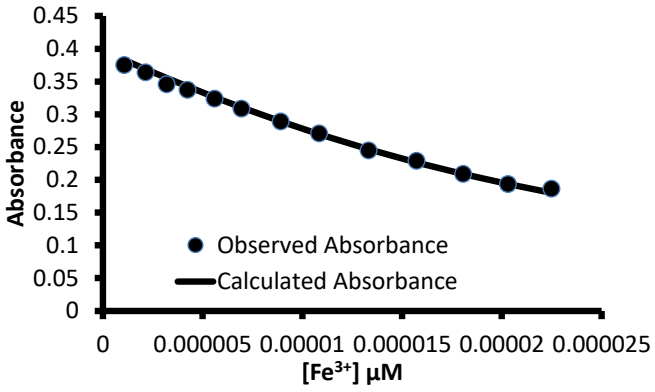

Figure S27. A correlation between the observed absorbance and absorbance value calculated using the HypSpec program for a titration between **1** and ferric ions with 1:1 (H:G) binding stoichiometry.

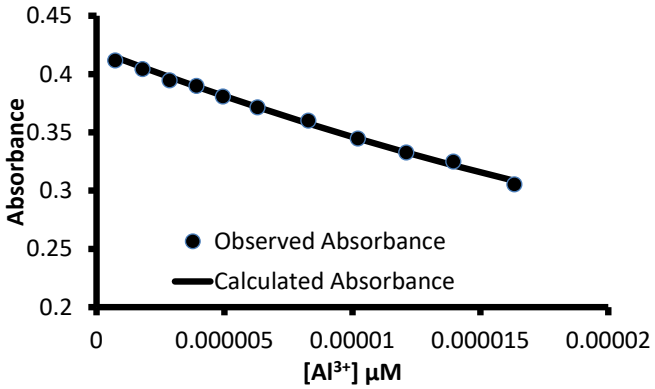

Figure S28. A correlation between the observed absorbance and absorbance value calculated using the HypSpec program for a titration between **1** and aluminum ions with 1:1 (H:G) binding stoichiometry.

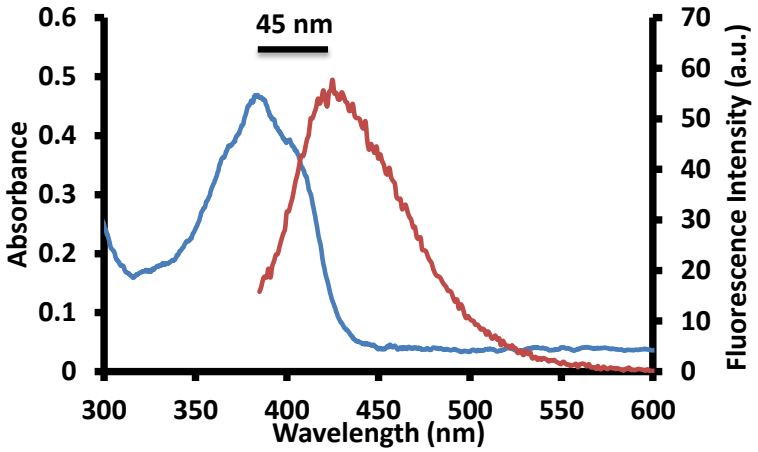

Figure S29. A comparison of the absorbance and fluorescence intensity for an equimolar solution of **1** and the mercuric ions.

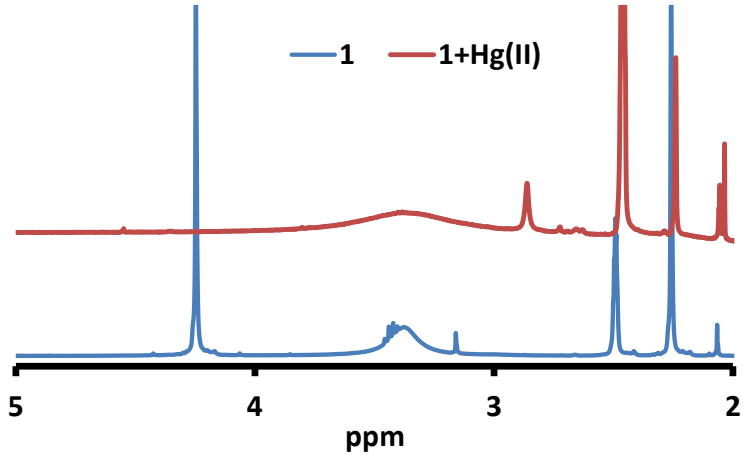

Figure S30. A partial ^{1}H-NMR spectra of **1** and **1**-Hg^{2+} showing a comparison in the aliphatic region. The ^{1}H-NMR spectra was recorded in DMSO-d_6 on a 400 MHz instrument.

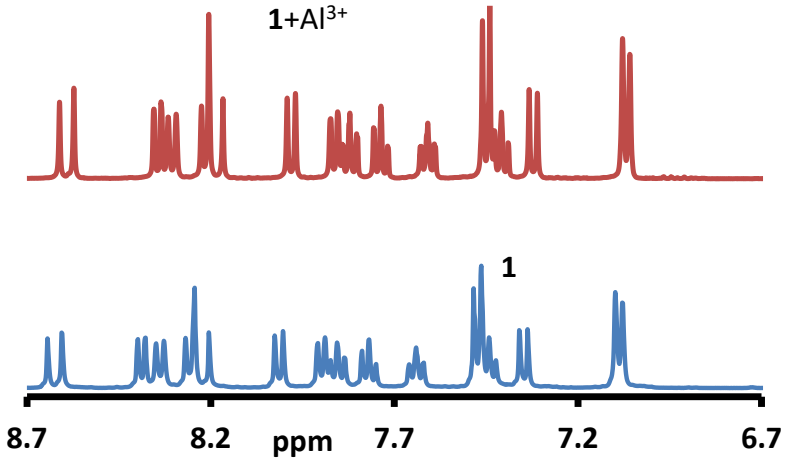

Figure S31. A partial ^{1}H-NMR spectra of **1** and **1**-Al^{3+} showing a comparison in the aromatic region. The ^{1}H-NMR spectra was recorded in DMSO-d_6 on a 400 MHz instrument.

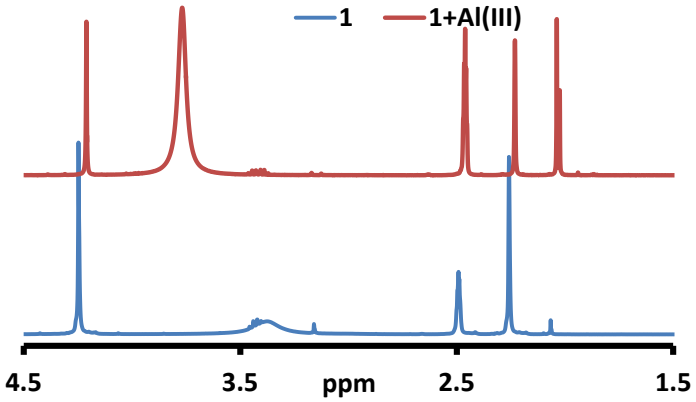

Figure S32. A partial ^{1}H-NMR spectra of **1** and **1**-Al^{3+} showing a comparison in the aliphatic region. The ^{1}H-NMR spectra was recorded in DMSO-d_6 on a 400 MHz instrument.

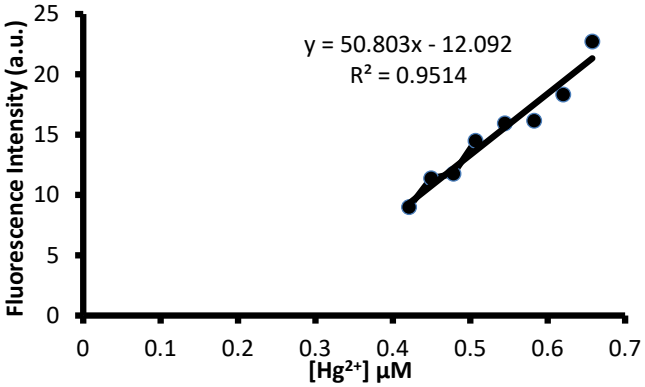

Figure S33. The determination of limit of detection value of **1** towards mercuric ions using fluorescence spectroscopy.

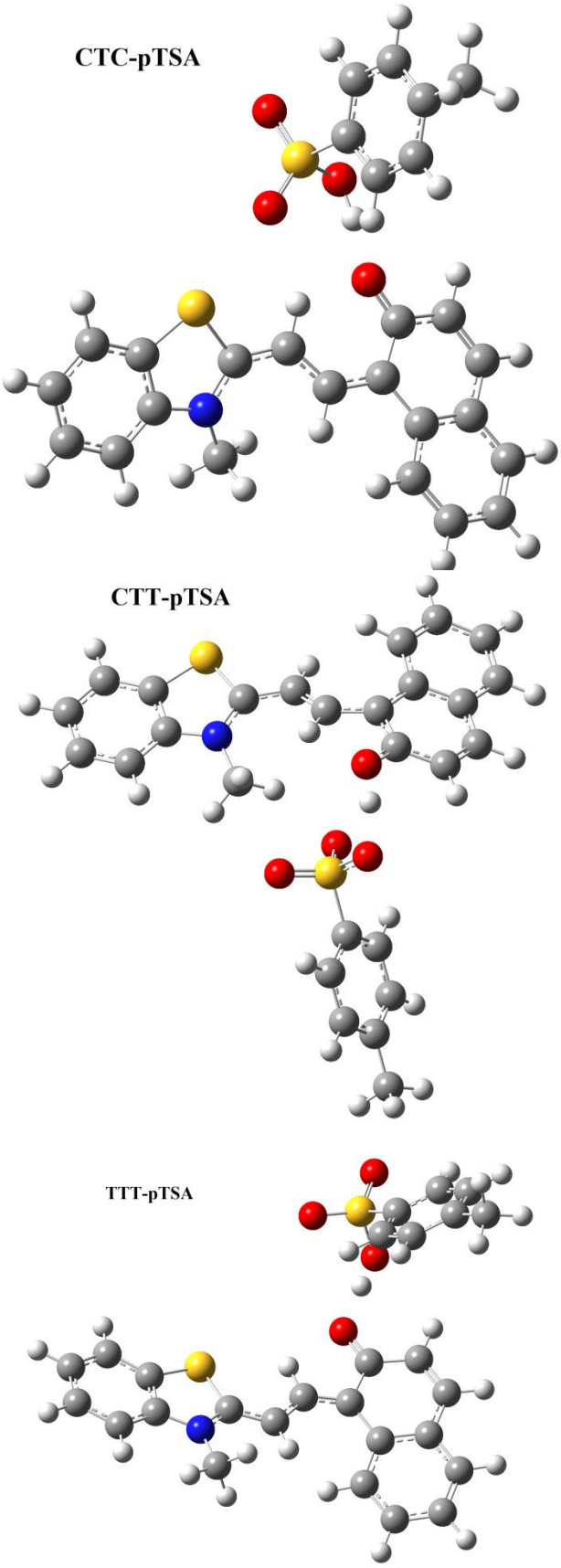

Figure S34. The DFT/PBE1PBE/6-31+G(d) optimized geometries of the different stereoisomers of **1**.

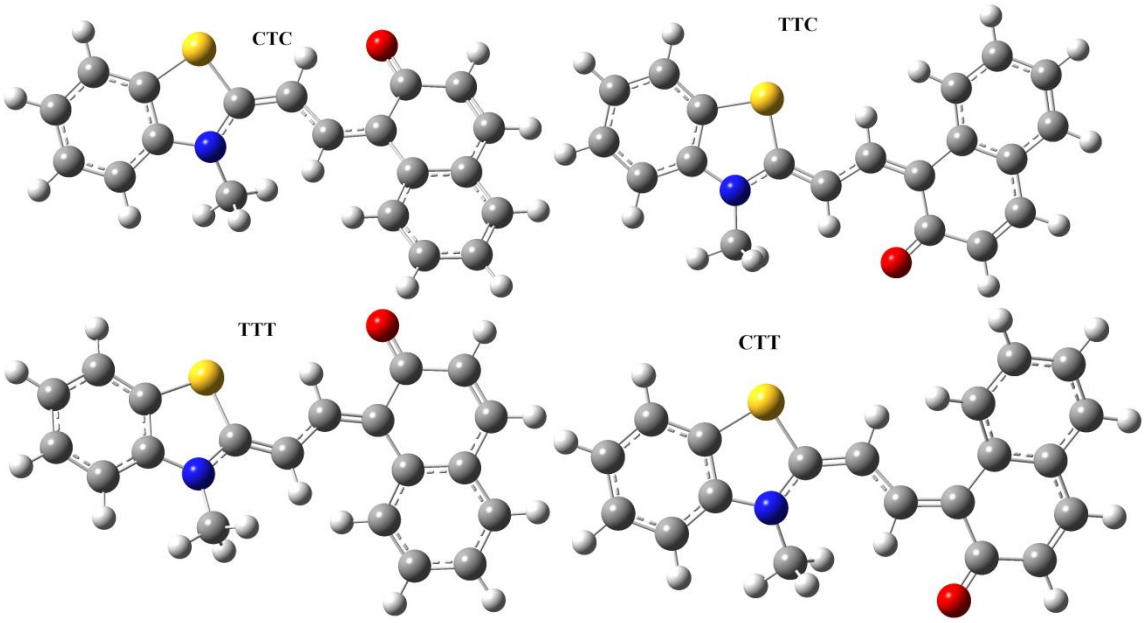

Figure S35. The DFT/PBE1PBE/6-31+G(d) optimized geometries of the different stereoisomers of **1** in the zwitterionic form.

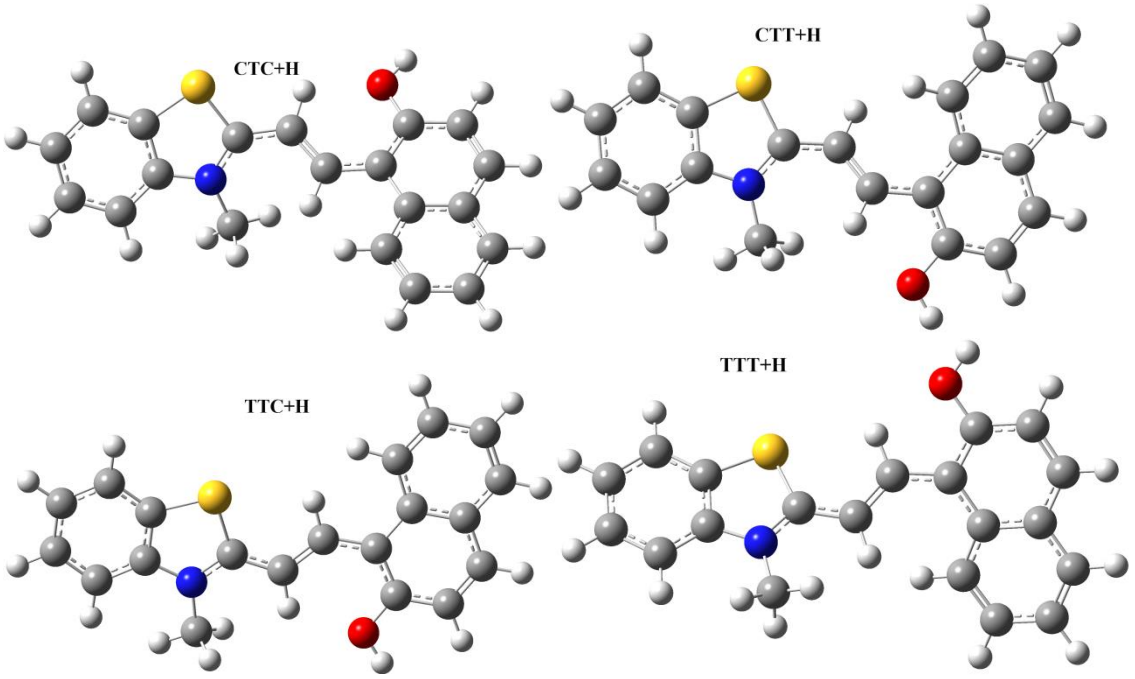

Figure S36. The DFT/PBE1PBE/6-31+G(d) optimized geometries of the different stereoisomers of **1** in the protonated form.

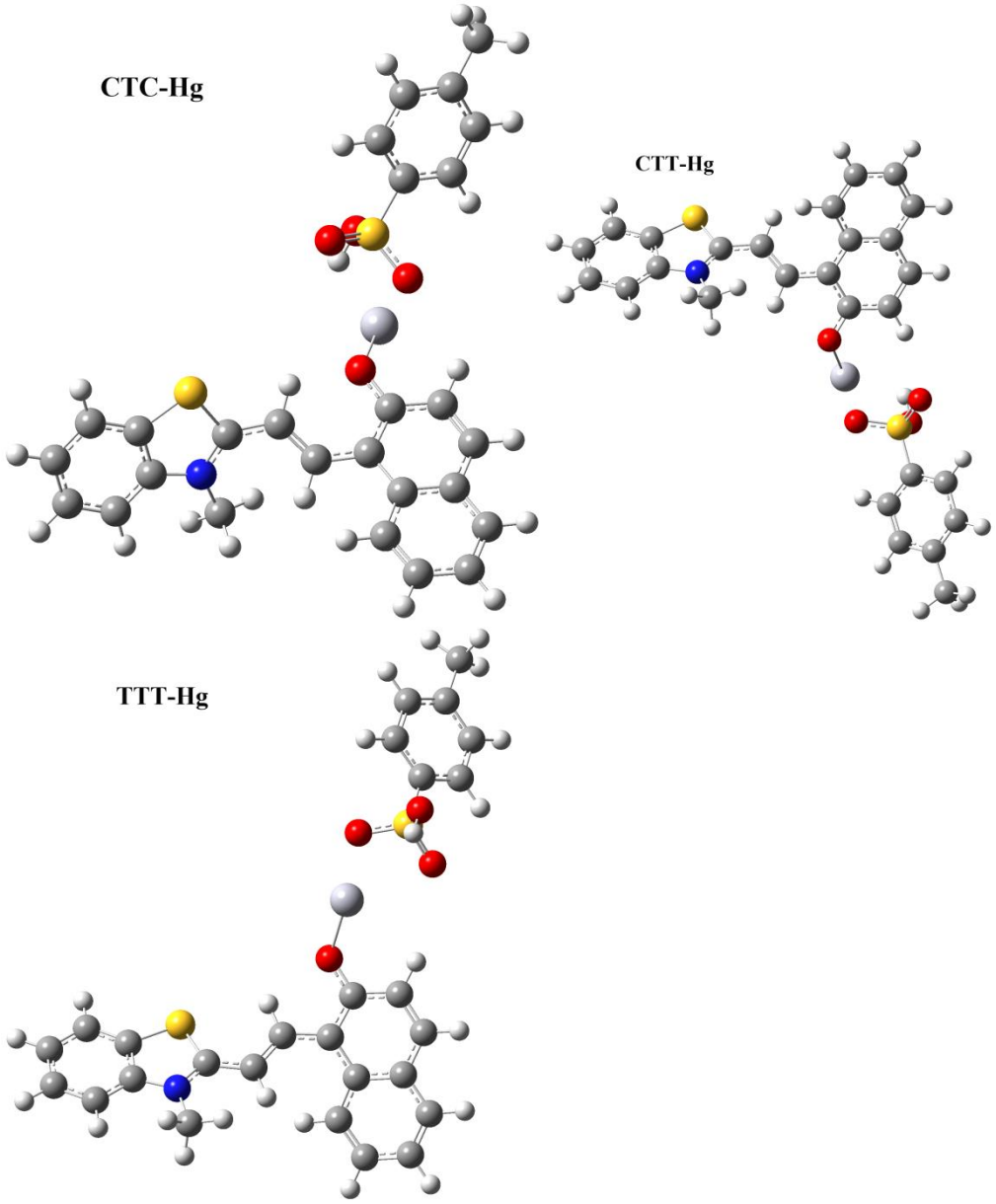

Figure S37. The DFT/PBE1PBE/6-31+G(d)/LANL2DZ optimized geometries of the **1**-Hg complex.

Table S3. The electronic excitation parameters for the receptors **1** and **1**-Hg^{2+} complex obtained calculated using TD-DFT/B3LYP/6-31G(d) method (Gaussian 09 A.02) in the gas phase.

		CIC	E(eV) [λ(nm)]	μ_x	μ_y	μ_z	μ_{total}	f
1	So to S1	H to L (0.70)	2.62 eV (473.73)	-1.72	8.19	-0.27	27.58	0.6957
1-Hg	Excited State 6	H to L+1 (0.67) H-2 to L+1 (0.16)	2.68 eV (463.05)	-3.79	6.14	0.11	20.52	0.5296
1-Hg	Excited State 9	H-1 to L+1 (0.68)	3.21 eV (385.74)	1.51	2.74	-0.02	3.84	0.1191